JOURNAL OF COMPUTATIONAL AND APPLIED MATHEMATICS

ELSEVIER Journal of Computational and Applied Mathematics 107 (1999) 31–52

On the zeroes of the Pearcey integral

D. Kaminski[a, *, 1], R.B. Paris[b]

[a] *Department of Mathematics and Computer Science, University of Lethbridge, 4401 University Drive, Lethbridge, Alta., Canada T1K 3M4*

[b] *Division of Mathematical Sciences, University of Abertay Dundee, Dundee DD1 1HG, UK*

Received 16 December 1998

Abstract

Zeroes for real values of the arguments of the Pearcey integral are numerically evaluated and plotted. From this numerical examination, it is apparent that these zeroes display a high degree of structure, the character of which is revealed through asymptotic analysis. Refinements to the resulting approximations are supplied near the paper's end. © 1999 Elsevier Science B.V. All rights reserved.

Keywords: Asymptotic expansion; Pearcey integral; Zero

1. Introduction

The Pearcey integral,

$$P(x, y) = \int_{-\infty}^{\infty} \exp(\mathrm{i}(t^4 + xt^2 + yt))\,\mathrm{d}t,$$

for real x and y, is one of a number of 'diffraction integrals' belonging to the same class of integrals as that defining the Airy function, and is used in work in optics [1] as well as in the asymptotics of special functions, especially uniform asymptotics [5] [7, Ch. VII, Section 6]. In 1982, Connor and Curtis presented a short table in [2] giving the zeroes of the Pearcey integral for x and y constrained to a small rectangle. In that same paper, they also supplied a modest table of values of P, P_x and P_y which was further extended in [3].

* Corresponding author.
E-mail address: kaminski@cs.uleth.ca (D. Kaminski)

[1] Research partially supported by NSERC of Canada.

PII: S0377-0427(99)00074-6

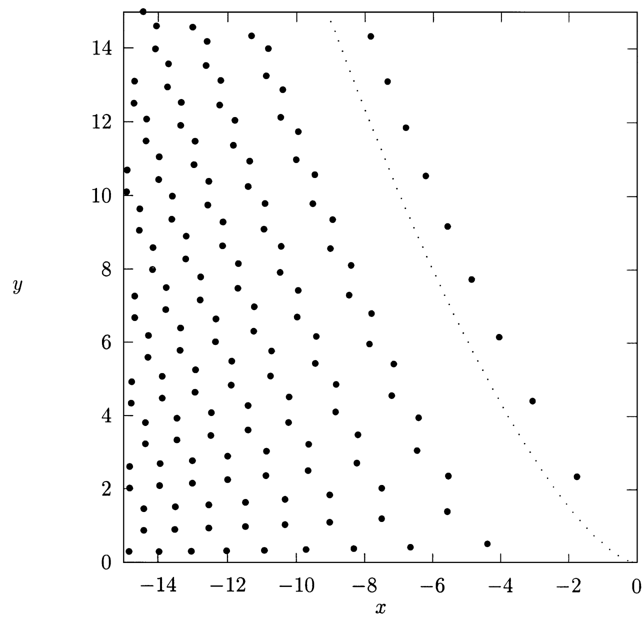

Fig. 1. Zeroes (heavier dots) of $P(x, y)$ in $[-15, 0] \times [0, 15]$. The caustic curve in this quadrant is indicated by a dotted arc.

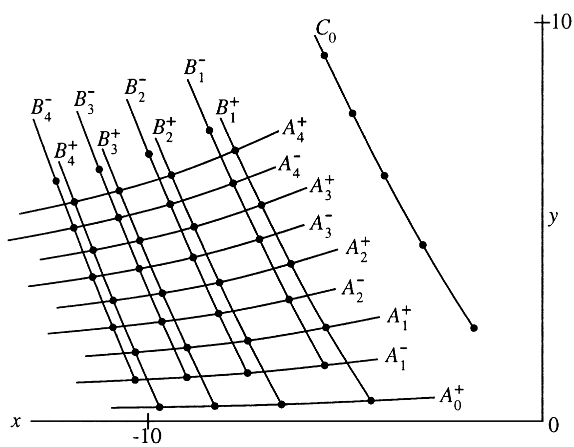

Fig. 2. The curves $A_n^{\pm}$, $B_n^{\pm}$ and C_0.

We recomputed the values of P, P_x and P_y to slightly greater precision over a much wider range of x and y, using the Netlib code `rksuite` and the scheme outlined in [4]. We also undertook an examination of the zeroes of the Pearcey function occurring in a rectangle of interest – $[-15, 0] \times [0, 15]$ – straddling the caustic, and observed interesting behaviour. Our numerically computed zeroes, plotted in Fig. 1, clearly fall into regular patterns. Above the caustic, there is a family of zeroes distributed along a curve of similar shape to that of the caustic. Below the caustic, the zeroes appear to be grouped into strands of pairs of zeroes. For ease of reference, we shall denote these families

Table 1
Zeroes in the strands C_0 and $B_1^{\pm}$

C_0		B_1^+		B_1^-	
x	y	x	y	x	y
−1.743600	2.352175	−4.378045	0.527678	−5.554698	1.411007
−3.057904	4.427072	−5.523207	2.360923	−6.446243	3.063888
−4.035513	6.161845	−6.403122	3.958046	−7.196286	4.565368
−4.848172	7.723520	−7.147179	5.422054	−7.857231	5.966693
−5.558322	9.173068	−7.804563	6.795357	−8.455299	7.294446
−6.196860	10.541385	−8.400332	8.100875	−9.005868	8.564701
−6.781814	11.846794	−8.949341	9.352752	−9.518882	9.788141
−7.324689	13.101373	−9.461264	10.560584	−10.001220	10.972330
−7.833398	14.313583	−9.942825	11.731230	−10.457874	12.122879
		−10.398922	12.869853	−10.892609	13.244106
		−10.833258	13.980425	−11.308344	14.339418

Table 2
Zeroes in the strands $B_2^{\pm}$

B_2^+		B_2^-	
x	y	x	y
−6.642850	0.430390	−7.499057	1.216048
−7.486288	2.029210	−8.223145	2.711928
−8.203264	3.492847	−8.863488	4.108220
−8.839042	4.864907	−9.444444	5.431366
−9.416818	6.168698	−9.980363	6.697354
−9.950403	7.418633	−10.480565	7.916806
−10.448826	8.624411	−10.951520	9.097241
−10.918385	9.792941	−11.397929	10.244242
−11.363678	10.929428	−11.823352	11.362095
−11.788193	12.037882	−12.230554	12.454190
−12.194646	13.121471	−12.621736	13.523265
−12.585205	14.182812	−12.998690	14.571574

of zeroes by $A_k^{\pm}$, $B_k^{\pm}$ and C_0. The C_0 family of curves is that strand of zeroes above the caustic, the $B_k^{\pm}$ families lie below the caustic in strands 'parallel' to the caustic, and the $A_k^{\pm}$ families refer to the $B_k^{\pm}$ families of zeroes grouped into strands that eventually appear to be 'parallel' to the negative x-axis. With these conventions, our zeroes appear to be distributed along the families depicted in Fig. 2.

The computed zeroes for the strands depicted in the rectangle $[-15,0]\times[0,15]$ are presented in Tables 1–5.

Table 3
Zeroes in the strands $B_3^{\pm}$

B_3^+		B_3^-	
x	y	x	y
−8.319160	0.384881	−9.025776	1.108799
−9.018457	1.849072	−9.652060	2.502903
−9.639922	3.220944	−10.221212	3.823907
−10.205641	4.524166	−10.746944	5.087812
−10.728793	5.773290	−11.238174	6.305242
−11.218016	6.978093	−11.701105	7.483722
−11.679340	8.145564	−12.140258	8.628825
−12.117178	9.280944	−12.559055	9.744840
−12.534882	10.388240	−12.960159	10.835150
−12.935065	11.470660	−13.345695	11.902493
−13.319815	12.530816	−13.717387	12.949119
−13.690831	13.570830	−14.076663	13.976910
−14.049520	14.592513	−14.424716	14.987461

Table 4
Zeroes in the strands $B_4^{\pm}$ and $B_5^{\pm}$

B_4^+		B_4^-	
x	y	x	y
−9.711669	0.356309	−10.327067	1.036718
−10.322182	1.728447	−10.887018	2.356570
−10.878606	3.031567	−11.404760	3.619289
−11.393670	4.280360	−11.888922	4.835523
−11.875722	5.484689	−12.345508	6.012804
−12.330601	6.651589	−12.778900	7.156720
−12.762584	7.786306	−13.192419	8.271560
−13.174920	8.892889	−13.588654	9.360714
−13.570146	9.974582	−13.969667	10.426915
−13.950291	11.033973	−14.337137	11.472417
−14.317007	12.073200	−14.692453	12.499107
−14.671661	13.094102		
B_5^+		B_5^-	
−10.928626	0.335922	−11.480968	0.983301
−11.477412	1.639195	−11.992075	2.245316
−11.985799	2.887924	−12.470345	3.460801
−12.461911	4.092041	−12.921624	4.637305
−12.911433	5.258619	−13.350188	5.780428
−13.338535	6.392959	−13.759273	6.894468
−13.746385	7.499109	−14.151405	7.982815
−14.137460	8.580306	−14.528601	9.048214
−14.513740	9.639170	−14.892504	10.092918
−14.876840	10.677877		

Table 5
Zeroes in the strands $B_6^{\pm}$, $B_7^{\pm}$ and $B_8^{\pm}$

B_6^+		B_6^-	
x	y	x	y
−12.023236	0.320285	−12.528640	0.941323
−12.525905	1.569112	−13.001831	2.156336
−12.996914	2.773187	−13.448525	3.332328
−13.441824	3.939624	−13.872905	4.474907
−13.864714	5.073727	−14.278142	5.588384
−14.268685	6.179613	−14.666709	6.676154
−14.656164	7.260490		
B_7^+		B_7^-	
−13.026293	0.307717	−13.495004	0.907012
−13.492815	1.511857	−13.937646	2.082668
−13.933659	2.678266	−14.358323	3.224876
−14.352830	3.812269	−14.760147	4.337951
−14.753371	4.917972		
B_8^+		B_8^-	
−13.957511	0.297281	−14.396515	0.878167
−14.394712	1.463736	−14.813862	2.020124
−14.810544	2.597718		

2. Approximate location of the zeroes inside the caustic

2.1. The case of large $|x|$ and bounded y

Let us first address the situation where $|x|$ is large and y is small relative to x. In this setting, the zeroes of $P(x, y)$ display a high degree of regularity in their distribution in the xy-plane, $x < 0$, as evidenced by Fig. 3.

Recall the asymptotic form presented in [6] (where the Pearcey function is denoted by $P'(X, Y)$),

$$P(x,y) \sim \sqrt{\frac{\pi}{|x|}}\,\mathrm{e}^{-\pi\mathrm{i}/4}\{S_1(|x|\mathrm{e}^{3\pi\mathrm{i}/4}, y\mathrm{e}^{\pi\mathrm{i}/8}) + \mathrm{i}\sqrt{2}\,\mathrm{e}^{-\mathrm{i}x^2/4}S_2(|x|\mathrm{e}^{3\pi\mathrm{i}/4}, y\mathrm{e}^{\pi\mathrm{i}/8})\}$$

$$\sim \sqrt{\frac{\pi}{|x|}}\,\mathrm{e}^{-\pi\mathrm{i}/4}\{1 + \mathrm{i}\sqrt{2}\,\mathrm{e}^{-\mathrm{i}x^2/4}\cos(y\sqrt{|x|/2})\}$$

with

$$S_1(x,y) = \mathrm{e}^{-y^2/4x}(1 + \mathcal{O}(1/x^2)),$$

$$S_2(x,y) = \tilde{P}(0,\xi)\cos\xi - \tilde{Q}(0,\xi)\sin\xi, \quad \xi = y\sqrt{-x/2}.$$

Set $P(x, y) = 0$ so that

$$\sqrt{\frac{\pi}{|x|}}\mathrm{e}^{-\pi\mathrm{i}/4}\{1 + \mathrm{i}\sqrt{2}\,\mathrm{e}^{-\mathrm{i}x^2/4}\cos(y\sqrt{|x|/2})\} \sim 0,$$

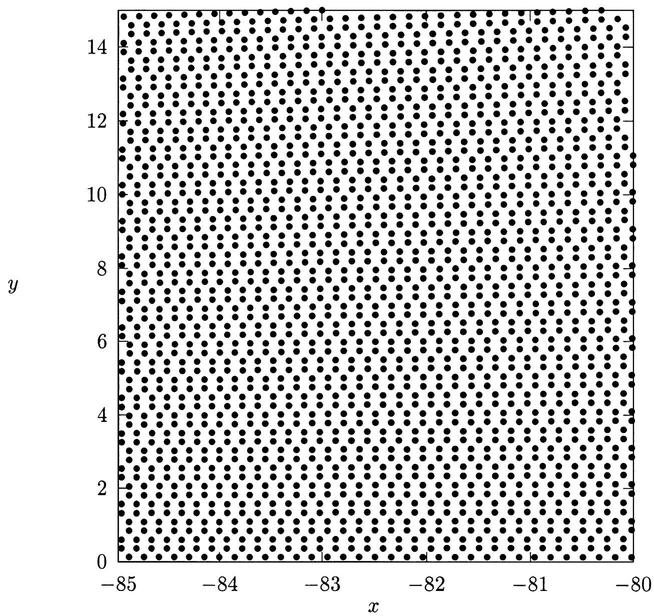

Fig. 3. Zeroes of $P(x,y)$ in $[-85,-80]\times[0,15]$.

or, upon separating real and imaginary parts,

$$\sin(x^2/4)\cos(y\sqrt{|x|/2}) = -1/\sqrt{2},$$
$$\cos(x^2/4)\cos(y\sqrt{|x|/2}) = 0.$$

The second equation implies that, if $\cos(x^2/4)=0$, then

$$\frac{x^2}{4} = (k+\tfrac{1}{2})\pi, \quad k=0,1,2,\ldots,$$

whence $x=x_k=-\sqrt{2(2k+1)\pi}$, $k=0,1,2,\ldots$ (we take $x<0$). For this x, we have $\sin(x^2/4)=(-1)^k$.

Because $\sin(x_k^2/4)=(-1)^k$, the first of the pair of equations reduces to

$$\cos(y\sqrt{|x_k|/2}) = (-1)^{k+1}/\sqrt{2}, \quad k=0,1,2,\ldots. \tag{2.1}$$

The angles for the cosine must therefore be $\pi/4, 3\pi/4, 5\pi/4,\ldots$, for which the alternation in sign is $+,-,-,+,+,\ldots$, respectively. Accordingly, for even k, we must have

$$y = \left(\frac{2l+1}{4}\right)\pi\sqrt{\frac{2}{|x_k|}} \tag{2.2}$$

for $l\equiv 1,2 \pmod 4$, with the same formula holding for odd k, but with $l\equiv 0,3 \pmod 4$.

For the range of values used in constructing Fig. 3, these approximate values for roots compare favourably with the computed roots, as presented in Table 6. It is evident in the table (and even more apparent in Fig. 3) that as y increases, the calibre of the approximation of the computed zeroes worsens.

Table 6
Computed versus approximate zeroes for large negative x and modest y

Computed zeroes		Approximate zeroes			
x	y	x	y	k	l
−82.032265	0.122633	−82.032259	0.122634	535	0
−82.032167	0.858442	−82.032259	0.858441		3
−82.032148	1.103707	−82.032259	1.103710		4
−82.031855	1.839522	−82.032259	1.839517		7
−82.031816	2.084784	−82.032259	2.084786		8
−82.031328	2.820611	−82.032259	2.820593		11
−82.108801	0.367732	−82.108817	0.367732	536	1
−82.108791	0.612883	−82.108817	0.612886		2
−82.108597	1.348352	−82.108817	1.348350		5
−82.108568	1.593503	−82.108817	1.593505		6
−82.108179	2.328978	−82.108817	2.328968		9
−82.108130	2.574127	−82.108817	2.574123		10

2.2. *Both $|x|$ and y large*

Let us return to the integral definition of $P(x,y)$,

$$P(-x,y)=\sqrt{x}\int_{-\infty}^{\infty}\exp(\mathrm{i}x^2(u^4-u^2+yx^{-3/2}u))\,\mathrm{d}u, \tag{2.3}$$

easily arrived at through a simple change of variable. Denoting the phase function of this integral by

$$\psi(u)=u^4-u^2+yx^{-3/2}u,$$

we have

$$\psi'(u)=4(u^3-u/2+yx^{-3/2}/4)$$

$$=4(u^3-(u_1+u_2+u_3)u^2+(u_1u_2+u_1u_3+u_2u_3)u-u_1u_2u_3)$$

where the roots of $\psi'(u)=0$ are indicated by u_1, u_2 and u_3. The elementary theory of equations furnishes us with

$$\sum u_i=0,\quad \sum_{i<j}u_iu_j=-1/2,\quad u_1u_2u_3=-yx^{-3/2}/4, \tag{2.4}$$

from which we deduce that one $u_i<0$, and the other two are positive. Let us label these so that, inside the caustic, we have

$$u_1<0<u_2<u_3. \tag{2.5}$$

We mention here that the theory of equations provides a trigonometric form for the roots u_i, namely,

$$\begin{aligned} u_1 &= -\sqrt{2/3}\sin(\phi+\pi/3), \\ u_2 &= \sqrt{2/3}\sin\phi, \\ u_3 &= \sqrt{2/3}\sin(\pi/3-\phi), \end{aligned} \tag{2.6}$$

where the angle ϕ is given by

$$\sin(3\phi) = \tfrac{3}{4}\sqrt{6}\,yx^{-3/2} \tag{2.7}$$

for $(-x, y)$ inside the caustic, guaranteeing real values of ϕ, and with $y > 0$, the order of the u_i remains as in Eq. (2.5). The zeroes displayed in Eq. (2.6) undergo a confluence when the angle ϕ defined in Eq. (2.7) tends to $\pi/6$. The curve this value of ϕ defines is the familiar caustic in the real plane: $y/x^{3/2} = (2/3)^{3/2}$.

The saddles u_i are therefore, respectively, the locations of a local minimum, a local maximum and a local minimum of ψ. Note, too, that a lower degree expression for the value of ψ at the critical points is available to us, namely

$$\psi(u_i) = -\tfrac{1}{2}u_i^2 + \tfrac{3}{4}yx^{-3/2}u_i, \tag{2.8}$$

which follows from $\psi'(u_i) = 0$. We shall have occasion to exploit this later.

For real x and y, we may rotate the contour of integration in Eq. (2.3) onto the line from $\infty e^{9\pi i/8}$ to $\infty e^{\pi i/8}$ through an application of Jordan's lemma. Since there are three real saddle points for $(-x, y)$ inside the caustic, we may further represent $P(-x, y)$ as a sum of three contour integrals,

$$P(-x, y) = \sqrt{x}\sum_{j=1}^{3}\int_{\Gamma_j} e^{ix^2\psi(u)}\,du, \tag{2.9}$$

where the contours Γ_j are the steepest descent curves: Γ_1, beginning at $\infty e^{9\pi i/8}$, ending at $\infty e^{5\pi i/8}$ and passing through $u_1 < 0$; Γ_2, beginning at $\infty e^{5\pi i/8}$, ending at $\infty e^{-3\pi i/8}$ and passing through $u_2 > 0$; and Γ_3, beginning at $\infty e^{-3\pi i/8}$, ending at $\infty e^{\pi i/8}$ and passing through $u_3 > u_2$. The general situation is depicted in Fig. 4. Let us set

$$d_1 = \sqrt{6u_1^2 - 1}, \qquad d_2 = \sqrt{1 - 6u_2^2} \quad \text{and} \quad d_3 = \sqrt{6u_3^2 - 1}. \tag{2.10}$$

In accordance with steepest descents or stationary phase philosophy, we set $\psi(u) - \psi(u_j) = (-1)^{j+1} d_j^2 v^2$, $j = 1, 2, 3$, to find at each saddle point u_j,

$$v = (u - u_j)\left\{1 + \frac{4u_j(u-u_j)}{6u_j^2 - 1} + \frac{(u-u_j)^2}{6u_j^2 - 1}\right\}^{1/2}$$

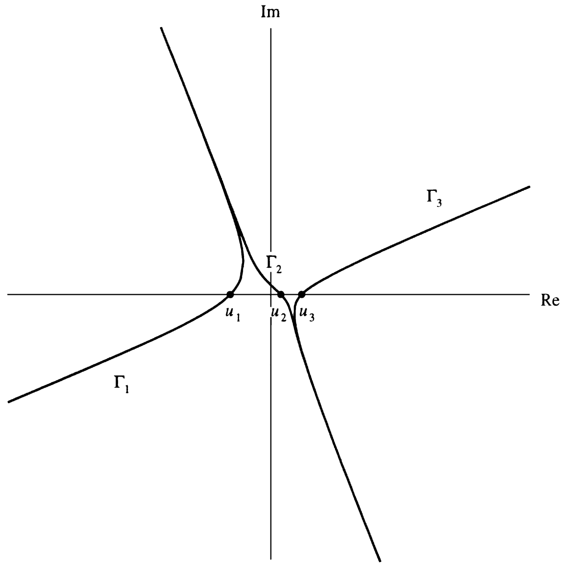

Fig. 4. Steepest descent curves through the saddles u_1, u_2 and u_3.

whence reversion yields the expansion, for each j,

$$u - u_j = \sum_{k=1}^{\infty} b_{k,j} v^k,$$

convergent in a neighbourhood of $v = 0$. We observe that $b_{1,j} = 1$ for each $j = 1, 2, 3$. Substitution into each term in Eq. (2.9) followed by termwise integration will furnish

$$\int_{\Gamma_j} \mathrm{e}^{\mathrm{i}x^2\psi(u)}\,\mathrm{d}u \sim \frac{\mathrm{e}^{(-1)^{j+1}\pi\mathrm{i}/4 + \mathrm{i}x^2\psi(u_j)}}{x d_j} \sum_{k=0}^{\infty} (2k+1) b_{2k+1,j} \frac{\Gamma(k+\frac{1}{2})((-1)^{j+1} i)^k}{x^{2k} d_j^{2k}},$$

so that

$$P(-x, y) \sim \sum_{j=1}^{3} \frac{\mathrm{e}^{\mathrm{i}x^2\psi(u_j) + (-1)^{j+1}\pi\mathrm{i}/4}}{d_j} \sqrt{\frac{\pi}{x}} \sum_{k=0}^{\infty} \frac{(2k+1) b_{2k+1,j}}{d_j^{2k}} \frac{\Gamma(k+\frac{1}{2})}{\Gamma(\frac{1}{2})} \frac{((-1)^{j+1} i)^k}{x^{2k}},$$

for large x.

For simplicity of presentation, let us write

$$a_{2k,j} = (-1)^{(j+1)k} \frac{(2k+1) b_{2k+1,j}}{d_j^{2k}} \frac{\Gamma(k+\frac{1}{2})}{\Gamma(\frac{1}{2})} \tag{2.11}$$

so that the above expansion of $P(-x, y)$ can be more compactly written

$$P(-x, y) \sim \sum_{j=1}^{3} \frac{\mathrm{e}^{\mathrm{i}x^2\psi(u_j) + (-1)^{j+1}\pi\mathrm{i}/4}}{d_j} \sqrt{\frac{\pi}{x}} \sum_{k=0}^{\infty} \frac{a_{2k,j} i^k}{x^{2k}}. \tag{2.12}$$

Each saddle point contributes an asymptotic series proportional to

$$\frac{e^{ix^2\psi(u_j)}}{d_j}\left\{1+\sum_{k=1}^{\infty}\frac{i^k a_{2k,j}}{x^{2k}}\right\}\equiv\frac{e^{iA_j}}{D_j},$$

where we put

$$A_j=x^2\psi(u_j)+\psi_j \quad \text{and} \quad D_j=d_j/(1+s_j)$$

with

$$\psi_j=\arg\left\{1+\sum_{k=1}^{\infty}\frac{i^k a_{2k,j}}{x^{2k}}\right\}=\frac{a_{2,j}}{x^2}+\mathcal{O}(x^{-4}),$$

$$1+s_j=\left|1+\sum_{k=1}^{\infty}\frac{i^k a_{2k,j}}{x^{2k}}\right|=1+\frac{(a_{4,j}+\frac{1}{2}a_{2,j}^2)}{x^4}+\mathcal{O}(x^{-8}).$$

From this it is apparent that

$$s_j=\frac{(a_{4,j}+\frac{1}{2}a_{2,j}^2)}{x^4}+\mathcal{O}(x^{-8})$$

and direct computation produces

$$a_{2,j}=\frac{1}{4d_j^4}\left(7+\frac{10}{(6u_j^2-1)}\right).$$

2.2.1. Zeroth order approximation

From Eq. (2.12), we have

$$P(-x,y)\sim\sqrt{\frac{\pi}{x}}\sum_{j=1}^{3}e^{(-1)^{j+1}\pi i/4}\frac{e^{iA_j}}{D_j}$$

which, to leading order, yields the approximation

$$P(-x,y)\sim\sqrt{\frac{\pi}{x}}\left\{\frac{e^{iA_1+\pi i/4}}{d_1}+\frac{e^{iA_2-\pi i/4}}{d_2}+\frac{e^{iA_3+\pi i/4}}{d_3}\right\}$$

in view of the fact $1/D_j\sim 1/d_j$, $j=1,2,3$. Upon setting real and imaginary parts of this approximation to zero, we find that zeroes $(-x,y)$ of P must satisfy (approximately) the pair of equations

$$\frac{\cos A_1}{d_1}+\frac{\sin A_2}{d_2}+\frac{\cos A_3}{d_3}=0, \tag{2.13}$$

$$\frac{\sin A_1}{d_1}-\frac{\cos A_2}{d_2}+\frac{\sin A_3}{d_3}=0; \tag{2.14}$$

recall that, to a first approximation, $A_j\sim x^2\psi(u_j)$. For the remainder of this section, we shall write A_j for $x^2\psi(u_j)$.

Isolate the terms involving $\sin A_2$ and $\cos A_2$, square the results and add to obtain

$$\frac{1}{d_2^2}-\frac{1}{d_1^2}-\frac{1}{d_3^2}=\frac{1}{d_1d_3}(2\cos A_1\cos A_3+2\sin A_1\sin A_3). \tag{2.15}$$

If one views the left-hand side of this equation in terms of the u_j, it becomes apparent that the result is a symmetric function of the u_j. Consequently, it is possible to evaluate the left-hand side of this equation in terms of the coefficients of $\psi'(u)=0$. To that end, we remark that equations (2.4) allow one to easily conclude that

$$\sum u_i^2 = 1 \quad \text{and} \quad \sum_{i<j} u_i^2 u_j^2 = 1/4,$$

from which we find, restoring the u_j, that

$$\begin{aligned}
\frac{1}{d_2^2} - \frac{1}{d_1^2} - \frac{1}{d_3^2} &= \frac{1}{1-6u_2^2} + \frac{1}{1-6u_1^2} + \frac{1}{1-6u_3^2} \\
&= \frac{1}{\prod(1-6u_i^2)}(3 - 12(u_1^2+u_2^2+u_3^2) + 36(u_1^2u_2^2 + u_1^2u_3^2 + u_2^2u_3^2)) \\
&= 0. \qquad (2.16)
\end{aligned}$$

We find, therefore, that Eq. (2.15) reduces to the more attractive form

$$0 = \cos(A_1 - A_3)$$

whence

$$A_3 - A_1 \doteq (k + \tfrac{1}{2})\pi \qquad (2.17)$$

for integral k. It is a straightforward matter to show that $A_3 - A_1 > 0$ using Eq. (2.8) and the first equation of (2.4):

$$\begin{aligned}
A_3 - A_1 &= x^2(\psi(u_3) - \psi(u_1)) \\
&= x^2(-\tfrac{1}{2}(u_3^2 - u_1^2) + \tfrac{3}{4}yx^{-3/2}(u_3 - u_1)) \\
&= x^2(u_3 - u_1)(-\tfrac{1}{2}(u_1 + u_3) + \tfrac{3}{4}yx^{-3/2}) \\
&= x^2(u_3 - u_1)(\tfrac{1}{2}u_2 + \tfrac{3}{4}yx^{-3/2}).
\end{aligned}$$

In view of the ordering of the saddle points (2.5), we see that each factor in the last line is positive. Therefore, in Eq. (2.17), we cannot have negative k whence

$$A_1 = A_3 - \pi(k + \tfrac{1}{2}), \quad k = 0, 1, 2, \ldots . \qquad (2.18)$$

With (2.18) in hand, we observe that

$$\cos A_1 = (-1)^k \sin A_3 \quad \text{and} \quad \sin A_1 = -(-1)^k \cos A_3,$$

so that the system (2.13)–(2.14) reduces to

$$\frac{(-1)^k \sin A_3}{d_1} + \frac{\cos A_3}{d_3} = -\frac{\sin A_2}{d_2}, \qquad (2.19)$$

$$\frac{(-1)^k \cos A_3}{d_1} - \frac{\sin A_3}{d_3} = -\frac{\cos A_2}{d_2}. \qquad (2.20)$$

Let us set

$$\tan\alpha = d_1/d_3, \qquad \sin\alpha = d_1/\sqrt{d_1^2+d_3^2}, \qquad \cos\alpha = d_3/\sqrt{d_1^2+d_3^2}. \tag{2.21}$$

Notice that since $u_1 < 0 < u_2 < u_3$ and since $\sum u_j = 0$, the product $(u_1-u_3)\cdot(-u_2) = (u_1-u_3)\cdot(u_1+u_3) = u_1^2 - u_3^2$ must be positive from which it follows $d_1 > d_3$ and so $\tan\alpha > 1$.

In view of Eq. (2.16) and the fact

$$\frac{d_1 d_3}{d_2\sqrt{d_1^2+d_3^2}} = \frac{(1/d_2)}{\sqrt{1/d_1^2+1/d_3^2}} = 1$$

we find that the system (2.19)–(2.20) becomes

$$(-1)^k \sin A_3 \cos\alpha + \cos A_3 \sin\alpha = -\sin A_2, \tag{2.22}$$

$$(-1)^k \cos A_3 \cos\alpha - \sin A_3 \sin\alpha = -\cos A_2. \tag{2.23}$$

We distinguish cases according to the parity of k.

If k is even, system (2.22)–(2.23) reduces to

$$\sin(A_3+\alpha) = -\sin A_2 = \sin(A_2+\pi),$$

$$\cos(A_3+\alpha) = -\cos A_2 = \cos(A_2+\pi),$$

from which it follows that

$$A_2 - A_3 = \alpha + (2j+1)\pi \tag{2.24}$$

for integral j.

If k is odd, system (2.22)–(2.23) reduces to

$$\sin(A_3-\alpha) = \sin A_2, \qquad \cos(A_3-\alpha) = \cos A_2.$$

Each of these implies $A_3 - \alpha + 2\pi j = A_2$ or, with a suitable shift in the integer parameter j,

$$A_2 - A_3 = 2\pi - \alpha + 2\pi j. \tag{2.25}$$

We gather (2.24) and (2.25) together as

$$A_2 - A_3 = 2j\pi + \begin{cases} \pi+\alpha, & k \text{ even},\\ 2\pi-\alpha, & k \text{ odd}, \end{cases} \tag{2.26}$$

for integral j.

Recall the trigonometric form for the saddle points u_j given in Eqs. (2.6) and (2.7). Use of the expressions for u_2 and u_3 in $A_2 - A_3 = x^2(\psi(u_2)-\psi(u_3))$, and the application of the identity $\sin 3\theta = 3\cos^2\theta - \sin^3\theta$, leads to the expression

$$A_2 - A_3 = \frac{2x^2}{\sqrt{3}}\sin^2(\phi - \tfrac{\pi}{6})\cos(2\phi + \tfrac{\pi}{6}).$$

Substitution of Eq. (2.26) into the left-hand side of this results in the equation

$$\frac{2x^2}{\sqrt{3}}\sin^2(\phi-\tfrac{\pi}{6})\cos(2\phi+\tfrac{\pi}{6})=2j\pi+\begin{cases}\pi+\alpha, & k \text{ even},\\ 2\pi-\alpha, & k \text{ odd},\end{cases} \tag{2.27}$$

which will be useful in what follows.

Again, from the trigonometric forms for the u_j, we also have

$$A_3-A_1=\frac{x^2}{3}(\sin(\tfrac{\pi}{3}-\phi)+\sin(\tfrac{\pi}{3}+\phi))\,(\sin\phi+\sin 3\phi)$$

where Eq. (2.7) has entered in an essential way. Application of the identity $\sin(\frac{\pi}{3}-\theta)+\sin(\frac{\pi}{3}+\theta)=\sqrt{3}\cos\theta$ permits us to write

$$A_3-A_1=\frac{2x^2}{\sqrt{3}}\sin 2\phi\cos^2\phi$$

whence use of Eq. (2.17) yields

$$x^2=\frac{\sqrt{3}(k+\frac{1}{2})\pi}{2\sin 2\phi\cos^2\phi}.$$

The preceding equation, coupled with Eq. (2.27), leads to a nonlinear equation in ϕ which can be solved for numerically, viz.,

$$(k+\tfrac{1}{2})\,\frac{\sin^2(\phi-\frac{\pi}{6})\cos(2\phi+\frac{\pi}{6})}{\sin 2\phi\,\cos^2\phi}=2j+\begin{cases}1+\alpha/\pi, & k \text{ even},\\ 2-\alpha/\pi, & k \text{ odd},\end{cases} \tag{2.28}$$

with j, k nonnegative integers, and α is the angle in the range $[\pi/4,\pi/2]$ given by Eq. (2.21). The trigonometric ratio following the factor $(k+\frac{1}{2})$ on the left-hand side arises frequently enough that we will set

$$S(\phi)=\frac{\sin^2(\phi-\frac{\pi}{6})\cos(2\phi+\frac{\pi}{6})}{\sin 2\phi\,\cos^2\phi} \tag{2.29}$$

and use this in subsequent sections.

With ϕ determined from Eq. (2.28), the roots to $P(x,y)=0$ follow from

$$x=-\sqrt{\frac{\sqrt{3}\,(k+\frac{1}{2})\,\pi}{2\sin 2\phi\cos^2\phi}}, \tag{2.30}$$

$$y=\left(-\frac{2}{3}x\right)^{3/2}\sin 3\phi; \tag{2.31}$$

recall Eq. (2.7). We note that, for j fixed, and k varying, we generate a strand of zeroes that is ‘parallel’ to the caustic (i.e., a $B_n^{\pm}$ strand of zeroes), whereas by fixing k and letting j vary, we generate zeroes from an $A_n^{\pm}$ strand.

Some indication of the quality of the approximate roots we obtain with Eqs. (2.28)–(2.31) can be seen by comparing the results of this scheme, presented for small values in Table 7, with tabulations of the computed zeroes displayed in Tables 1–5. The strands of zeroes B_1^{+} and B_1^{-}, for example, correspond to $j=0$ and $k=0,2,4,\ldots$ and $k=1,3,5,\ldots$, respectively.

Table 7
Approximate values of roots (x, y) of $P(x, y) = 0$ using (2.28)

$k \setminus j$	0	1	2	3
0	$\phi = 0.036111$	0.015467	0.0098417	0.0072171
	$-x = 4.3447$	6.6328	8.3140	9.7084
	$y = 0.53299$	0.43130	0.38522	0.35648
1	0.067107	0.036437	0.025097	0.019155
	5.5350	7.4917	9.0216	10.324
	1.4174	1.2177	1.1095	1.0371
2	0.11486	0.061186	0.041977	0.031991
	5.5018	7.4787	9.0143	10.319
	2.3728	2.0320	1.8503	1.7291
3	0.11786	0.071115	0.051370	0.040297
	6.4301	8.2169	9.6485	10.885
	3.0732	2.7146	2.5042	2.3573
4	0.15642	0.092420	0.066411	0.051984
	6.3851	8.1968	9.6363	10.876
	3.9718	3.4965	3.2226	3.0325

2.2.2. Higher order approximations

Now instead of using only the dominant term in the expression for A_j, let us retain all of A_j. Proceeding as before, we find

$$\frac{\cos A_1}{D_1} + \frac{\sin A_2}{D_2} + \frac{\cos A_3}{D_3} = 0, \tag{2.32}$$

$$\frac{\sin A_1}{D_1} - \frac{\cos A_2}{D_2} + \frac{\sin A_3}{D_3} = 0 \tag{2.33}$$

so that

$$\frac{1}{D_2^2} = \frac{1}{D_1^2} + \frac{1}{D_3^2} + \frac{2}{D_2 D_3}\cos(A_3 - A_1)$$

or

$$\cos(A_3 - A_1) = -\frac{D_1 D_3}{2}\left\{\frac{2s_1 + s_1^2}{d_1^2} + \frac{2s_3 + s_3^2}{d_3^2} - \frac{2s_2 + s_2^2}{d_2^2}\right\} \equiv \delta,$$

where use has been made of $1/d_1^2 + 1/d_3^2 = 1/d_1^2$. Thus,

$$A_3 - A_1 = (k + \tfrac{1}{2})\pi + (-1)^k \varepsilon, \quad \delta = \sin \varepsilon. \tag{2.34}$$

It is clear that δ, and hence ε, is $\mathcal{O}(x^{-4})$.

Continuing, we find

$$\cos A_1 = \cos(A_3 - ((k+\tfrac{1}{2})\pi + (-1)^k\varepsilon)) = -\cos A_3 \sin\varepsilon + (-1)^k \sin A_3 \cos\varepsilon,$$
$$\sin A_1 = \sin(A_3 - ((k+\tfrac{1}{2})\pi + (-1)^k\varepsilon)) = -\sin A_3 \sin\varepsilon - (-1)^k \cos A_3 \cos\varepsilon,$$

and Eqs. (2.32) and (2.33) yield

$$(-1)^k D_3 \sin A_3 \cos\varepsilon + \cos A_3(D_1 - D_3\sin\varepsilon) = -\frac{D_1D_3}{D_2}\sin A_2,$$

$$(-1)^k D_3 \cos A_3 \cos\varepsilon - \sin A_3(D_1 - D_3\sin\varepsilon) = -\frac{D_1D_3}{D_2}\cos A_2.$$

Observe that

$$\frac{D_1D_3}{D_2\sqrt{D_3^2\cos^2\varepsilon + (D_1 - D_3\sin\varepsilon)^2}} = \frac{D_1D_3}{D_2\sqrt{D_1^2 + D_3^2 - 2D_1D_3\delta}}$$
$$= \frac{1/D_2}{\sqrt{1/D_1^2 + 1/D_3^2 - 2\delta/D_1D_3}} = 1.$$

Use of this in the preceding system yields the appreciably simpler pair of equations

$$\begin{cases} \sin(A_3 \pm \alpha) = \mp \sin A_2, & k \text{ even}, \\ \cos(A_3 \pm \alpha) = \mp \cos A_2, & k \text{ odd}, \end{cases} \tag{2.35}$$

where we have set

$$\alpha = \arctan\left(\frac{D_1 - D_3\sin\varepsilon}{D_3\cos\varepsilon}\right). \tag{2.36}$$

This yields the same equations as before, namely for $j = 0, 1, \ldots,$

$$A_2 - A_3 = 2j\pi + \begin{cases} \alpha + \pi, & k \text{ even}, \\ 2\pi - \alpha, & k \text{ odd}. \end{cases} \tag{2.37}$$

In a fashion that parallels the setting of the zeroth order approximation, we observe that

$$A_3 - A_1 = \frac{2}{\sqrt{3}}x^2 \sin 2\phi \cos^2\phi + \psi_3 - \psi_1,$$

$$A_2 - A_3 = \frac{2}{\sqrt{3}}x^2 \sin^2(\phi - \tfrac{\pi}{6})\cos(2\phi + \tfrac{\pi}{6}) + \psi_2 - \psi_3,$$

so that Eqs. (2.34) and (2.37) yield

$$\frac{2}{\sqrt{3}}x^2 \sin 2\phi \cos^2\phi = (k+\tfrac{1}{2})\pi + (\psi_1 - \psi_3) + (-1)^k\varepsilon,$$

$$\frac{2}{\sqrt{3}}x^2 \sin^2(\phi - \tfrac{\pi}{6})\cos(2\phi + \tfrac{\pi}{6}) = 2j\pi + (\psi_3 - \psi_2) + \begin{cases} \alpha + \pi, & k \text{ even}, \\ 2\pi - \alpha, & k \text{ odd}. \end{cases}$$

Hence,

$$((k+\tfrac{1}{2})+\psi_1-\psi_3+(-1)^k\varepsilon)S(\phi)=2j\pi+(\psi_3-\psi_2)+\begin{cases}\alpha+\pi, & k \text{ even},\\ 2\pi-\alpha, & k \text{ odd},\end{cases} \tag{2.38}$$

where

$$\psi_1-\psi_3=\frac{(a_{2,1}-a_{2,3})}{x^2}+\mathcal{O}(x^{-4})\equiv\frac{\Delta_{13}}{x^2}+\mathcal{O}(x^{-4}),$$
$$\psi_3-\psi_2=\frac{(a_{2,3}-a_{2,2})}{x^2}+\mathcal{O}(x^{-4})\equiv\frac{\Delta_{32}}{x^2}+\mathcal{O}(x^{-4}).$$

Set $\alpha_0=\arctan(d_1/d_3)$ and write $\alpha=\alpha_0+\mathcal{O}(x^{-4})$. Develop ε and ϕ into Poincaré series,

$$\varepsilon=\frac{E_1}{x^4}+\frac{E_2}{x^6}+\cdots,$$
$$\phi=\phi_0+\frac{\phi_1}{x^2}+\frac{\phi_2}{x^4}+\cdots.$$

The Taylor series expansion of S produces an approximation

$$\begin{aligned}S(\phi)&=S(\phi_0)+\left(\frac{\phi_1}{x^2}+\frac{\phi_2}{x^4}+\cdots\right)S'(\phi_0)+\cdots\\ &=S(\phi_0)+\frac{\phi_1}{x^2}S'(\phi_0)+\mathcal{O}(x^{-4})\end{aligned}$$

which, when substituted into Eq. (2.38) along with the series for ε and ϕ, results in

$$(k+\tfrac{1}{2})\pi S(\phi_0)=2j\pi+\begin{cases}\alpha_0+\pi, & k \text{ even},\\ 2\pi-\alpha_0, & k \text{ odd},\end{cases}$$

$$(k+\tfrac{1}{2})\pi\frac{\phi_1}{x^2}S'(\phi_0)+\Delta_{13}S(\phi_0)=\Delta_{32}$$

from which we can conclude

$$\phi_1=\frac{\Delta_{32}-\Delta_{13}S(\phi_0)}{(k+\frac{1}{2})\pi S'(\phi_0)}.$$

This first term beyond ϕ_0 allows us to refine the approximate value of x through

$$\begin{aligned}x^2&=\frac{\sqrt{3}}{2}\frac{(k+\frac{1}{2})\pi}{\sin 2\phi\cos^2\phi}\left\{1+\frac{\psi_1-\psi_3+(-1)^k\varepsilon}{(k+\frac{1}{2})}\right\}\\ &=x_0^2\left\{1+\frac{\psi_1-\psi_3}{(k+\frac{1}{2})\pi}+\mathcal{O}(x^{-4})\right\}\cdot\left\{1-\frac{2\phi_1}{x^2}\cot 2\phi_0+\cdots\right\}\cdot\left\{1+\frac{2\phi_1}{x^2}\tan\phi+\cdots\right\}\end{aligned}$$

with

$$x_0^2 = \frac{\sqrt{3}(k+\frac{1}{2})\pi}{2\sin^2\phi_0\cos 2\phi_0},$$

$$y_0 = \left(\frac{2}{3}x_0\right)^{3/2}\sin 3\phi_0.$$

Continuing in this vein will generate a series expansion for x,

$$x \sim x_0\left\{1+\frac{f_1}{x_0^2}+\frac{f_2}{x_0^4}+\cdots\right\} \tag{2.39}$$

where

$$f_1 = \frac{\Delta_{13}}{2(k+\frac{1}{2})\pi}+\phi_1(2\tan\phi_0-\cot 2\phi_0)$$

$$= \frac{1}{(k+\frac{1}{2})\pi}\left\{\frac{1}{2}\Delta_{13}+\frac{(\Delta_{32}-\Delta_{13}S(\phi_0))}{S'(\phi_0)}(2\tan\phi_0-\cot 2\phi_0)\right\}.$$

Incorporating this into the corresponding equation for y produces

$$y = (\tfrac{2}{3}x)^{3/2}\sin 3\phi$$

$$= (\tfrac{2}{3}x_0)^{3/2}\left\{1+\frac{c_1}{x_0^2}+\cdots\right\}^{3/2}\sin 3\phi_0\left\{1+\frac{3\phi_1}{x_0^2}\cot 3\phi_0+\cdots\right\}$$

$$= (\tfrac{2}{3}x_0)^{3/2}\sin 3\phi_0\left\{1+\frac{3c_1}{2x_0^2}+\frac{3\phi_1}{x_0^2}\cot 3\phi_0+\cdots\right\}$$

so that it is seen that y also possesses a Poincaré series expansion of the form

$$y \sim y_0\left\{1+\frac{g_1}{x_0^2}+\frac{g_2}{x_0^4}+\cdots\right\} \tag{2.40}$$

with

$$g_1 = \frac{3}{2}c_1+3\phi_1\cot 3\phi_0.$$

The improvement gained in using higher order approximations can be seen from the numerical example presented in Table 8.

3. Approximate location of the zeroes outside the caustic

If $(-x,y)$, $x>0$, lies outside the caustic, then we must have $y/x^{3/2} > (2/3)^{3/2}$. Let us set

$$b = (\tfrac{2}{3})^{3/2}a = \frac{y}{x^{3/2}}$$

for $a>1$. The saddle points for the phase $\psi(u)$, i.e., the solutions to

$$u^3-\tfrac{1}{2}u+\tfrac{1}{4}b=0,$$

Table 8
Approximate zeroes using first order correction

k	j	Zeroth order values	Corrected values	Exact values
2	4	$\phi_0 = 0.0258546$		
		$x_0 = -11.475406$	$x = -11.477422$	-11.477412
		$y_0 = 1.639605$	$y = 1.639200$	1.639195
4	4	$\phi_0 = 0.0427547$		
		$x_0 = -11.983988$	$x = -11.985806$	-11.985799
		$y_0 = 2.888542$	$y = 2.887928$	2.887924
6	4	$\phi_0 = 0.0572645$		
		$x_0 = -12.460241$	$x = -12.461913$	-12.461911
		$y_0 = 4.0928088$	$y = 4.092041$	4.092041
8	4	$\phi_0 = 0.0699471$		
		$x_0 = -12.909870$	$x = -12.911429$	-12.461911
		$y_0 = 5.2595063$	$y = 5.258620$	5.258619
10	4	$\phi_0 = 0.0811888$		
		$x_0 = -13.3370554$	$x = -13.338525$	-13.338535
		$y_0 = 6.3939262$	$y = 6.392945$	6.392959
12	4	$\phi_0 = 0.0912661$		
		$x_0 = -13.744973$	$x = -13.746369$	-13.746385
		$y_0 = 7.50015$	$y = 7.499090$	7.499109
14	4	$\phi_0 = 0.100384$		
		$x_0 = -14.136103$	$x = -14.1374380$	-14.137460
		$y_0 = 8.5814121$	$y = 8.580286$	8.580306
6	6	$\phi_0 = 0.0430621$		
		$x_0 = -14.351771$	$x = -14.352830$	-14.352830
		$y_0 = 3.812672$	$y = 3.812274$	3.812269
8	6	$\phi_0 = 0.0533838$		
		$x_0 = -14.752371$	$x = -14.753369$	-14.753371
		$y_0 = 4.918452$	$y = 4.917987$	4.917972

could be obtained from Eqs. (2.6) and (2.7) for complex values of ϕ, but we elect instead to express the solutions of $\psi'(u) = 0$ using surds, so that roots are now given by

$$\begin{aligned} u_1 &= \sigma_1 + \sigma_2, \\ u_{2,3} &= -\tfrac{1}{2}u_1 \pm i\tfrac{\sqrt{3}}{2}(\sigma_1 - \sigma_2), \end{aligned} \tag{3.1}$$

where here the σ_j are given by

$$\sigma_1 = -\frac{1}{\sqrt{6}}(a - \sqrt{a^2-1})^{1/3} \quad \text{and} \quad \sigma_2 = -\frac{1}{\sqrt{6}}(a + \sqrt{a^2-1})^{1/3}.$$

An analysis of the steepest descent curves passing through the saddles u_1, u_2 and u_3 reveals a situation – depicted in Fig. 5 – in which only two steepest descent paths are used to represent $P(-x, y)$, unlike the case inside the caustic ($a < 1$) where the integration contour can be represented as a sum of three steepest descent paths; recall Fig. 4 and Eq. (2.9). The steepest descent expansion

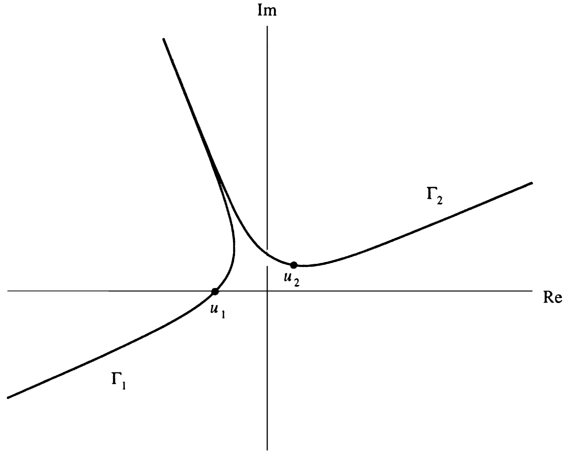

Fig. 5. Steepest descent curves through saddles when $(-x, y)$ lies outside the caustic. The third saddle point is the conjugate of u_2.

that yields an approximate value for $P(-x, y)$ is therefore similar to Eq. (2.12), except that instead of summing over three saddle point contributions, we have but two contributing to the expansion, which to leading terms provide the initial approximation

$$\frac{e^{ix^2\psi(u_1)}}{\sqrt{6u_1^2-1}} + \frac{e^{ix^2\psi(u_2)}}{\sqrt{6u_2^2-1}} = 0 \tag{3.2}$$

for a suitable branch of square root. Let us write

$$d_1 = \sqrt{6u_1^2-1} \quad \text{and} \quad d_2 e^{i\vartheta} = \sqrt{6u_2^2-1},\ d_2 > 0, \tag{3.3}$$

and

$$\psi(u_2) = -\tfrac{1}{2}u_2^2 + \tfrac{3}{4}bu_2 \equiv \psi_r + i\psi_i; \tag{3.4}$$

recall Eqs. (2.10) and (2.8). We can recast Eq. (3.2) as

$$\frac{e^{ix^2\psi(u_1)}}{d_1} + \frac{e^{ix^2\psi_i - x^2\psi_i}}{d_2 e^{i\vartheta}} = 0$$

which, upon looking at the modulus and phase of each term, results in

$$x^2\psi_i = \log(d_1/d_2) \quad \text{and} \quad e^{ix^2\psi(u_1)} + e^{ix^2\psi_r - i\vartheta} = 0. \tag{3.5}$$

The second of these equations yields

$$x^2(\psi_r - \psi(u_1)) = (2j+1)\pi + \vartheta$$

for j a nonnegative integer. That j should be so restricted is a consequence of the fact that, for real u and $(-x, y)$ outside the caustic, ψ has a global minimum at u_1 whence $\psi_r > \psi(u_1)$.

Solving for x^2 in Eq. (3.5) leads to the result

$$\log(d_1/d_2)\cdot(\psi_r - \psi(u_1)) = ((2j+1)\pi + \vartheta)\cdot\psi_i \tag{3.6}$$

Table 9
Approximate zeroes for $(-x, y)$ outside the caustic

	Approximate values			Computed values	
j	a	x_j	y_j	x_j	y_j
0	2.11305	1.62473	2.38202	1.743600	2.352175
1	1.59420	2.98251	4.46970	3.057904	4.427072
2	1.43872	3.97466	6.20569	4.035513	6.161845
3	1.35898	4.79507	7.76729	4.848172	7.723520
4	1.30904	5.51021	9.21652	5.558322	9.173068
5	1.27422	6.15234	10.58450	6.196860	10.541385

for j a nonnegative integer. Bear in mind that every quantity in Eq. (3.6) is ultimately a function of b or, equivalently, a, so that by setting j, we can use Eq. (3.6) to numerically determine suitable $a > 1$. Once such an a is in hand, we have

$$x_j = \sqrt{\frac{(2j+1)\pi + \vartheta}{\psi_{\rm r} - \psi(u_1)}} \quad \text{and} \quad y_j = a(\tfrac{2}{3}x_j)^{3/2} \tag{3.7}$$

to determine roots to $P(-x, y) = 0$. Some sample computations are supplied in the accompanying Table 9.

One could attempt to construct an analogue of the higher order approximation scheme as was done in Section 2.2.2, but for zeroes outside the caustic. In such an event, the reader will discover the computations are more daunting, in part because the third (complex) zero does not enter the computations and so removes an important tool for simplifying expressions, namely the elegant equations obtained from elementary symmetric functions. Instead of using the surd form for the u_j as we have done here, one could still use the trigonometric form (2.6), only now the angle ϕ would be complex, and the trigonometric functions would effectively be products of both trigonometric and hyperbolic functions. For these reasons, the quest for higher order approximate zeroes has been excluded from this discussion.

4. Conclusion

The approximation schemes for zeroes of the Pearcey function, both inside and outside the caustic, determined in this work (cf. (2.1)–(2.2),(2.30)–(2.31) and extensions in Section 2.2.2, Eq. (3.7)) are amenable to quick computation by machine and clearly reproduce the zeroes computed by the method of Connor et al. [2–4], even for moderately small values of the zeroes.

We remark that these schemes undergo considerable simplification under some circumstances. For example, if k is held fixed and j allowed to increase in (2.30)–(2.31), then we are in the setting considered in Section 2.1 and further, in view of (2.29), $S(\phi) \to \infty$ or equivalently, in the notation of Section 2.2.1, $\phi \to 0$ and $\alpha \to \pi/4$. Eq. (2.28) then reduces to

$$(k+\tfrac{1}{2})\frac{\sqrt{3}}{16\phi} \approx 2j + \tfrac{1}{4}(6 \mp 1)$$

whence

$$\phi \sim \frac{\sqrt{3}(k+\frac{1}{2})}{4(8j+6\mp 1)}$$

with the upper choice of sign for even k, and the lower choice for odd k.

With ϕ so obtained, the scheme (2.30)–(2.31) produces approximate solutions to $P(-x,y)=0$ of

$$x \approx \sqrt{\frac{\sqrt{3}(k+\frac{1}{2})\pi}{4\phi}} \approx \sqrt{\pi(8j+6\mp 1)},$$

$$y \approx \left(\tfrac{2}{3}x\right)^{3/2} 3\phi \approx \frac{(k+\frac{1}{2})\pi^{3/4}}{\sqrt{2}(8j+6\mp 1)^{1/4}}.$$

This approximation is effectively (2.1)–(2.2).

Were we to reverse the roles played by j and k and fix j and let k increase, we would find that now $S(\phi)$ is evanescent, or equivalently, $\phi \to \pi/6$ and $\alpha \to \pi/2$, so that x in Eq. (2.30) has the approximate behaviour

$$x \approx 2\sqrt{\tfrac{1}{2}\pi(k+\tfrac{1}{2})},$$

where $P(-x,y)=0$.

Continuing this line of investigation, let us set $\phi = \pi/6 - \varepsilon$ so that as k increases, $\varepsilon \to 0^+$. Eq. (2.31) and the above estimate for x immediately reduces to $y \approx y_0 \cos 3\varepsilon \approx y_0(1-\frac{9}{2}\varepsilon^2)$ where $y_0 = \left(\frac{4}{3}\sqrt{\frac{1}{2}\pi(k+\frac{1}{2})}\right)^{3/2}$. Furthermore, from $S(\phi) \approx 16\varepsilon^3/3\sqrt{3}$, Eq. (2.28) becomes

$$\left(k+\tfrac{1}{2}\right)\frac{16\varepsilon^3}{3\sqrt{3}} \approx 2j + \tfrac{3}{2},$$

which gives an approximate representation for ε in terms of j and k, viz.,

$$\varepsilon \approx \frac{\sqrt{3}}{2}\sqrt[3]{\frac{j+\frac{3}{4}}{k+\frac{1}{2}}}.$$

The approximate value of y therefore becomes

$$y \approx \frac{8}{3\sqrt{3}}\left(\tfrac{1}{3}\pi(k+\tfrac{1}{2})\right)^{3/4} \cdot \left(1 - \frac{27}{8}\left(\frac{j+\frac{3}{4}}{k+\frac{1}{2}}\right)^{2/3}\right).$$

Finally, we suppose j and k both tend to infinity as $j = mk$, where m is bounded. To leading order, Eq. (2.28) reduces to

$$S(\phi) = 2m + \mathcal{O}(k^{-1}).$$

$S(\phi)$ decreases monotonically from $+\infty$ (where ϕ vanishes) to zero at $\phi=\pi/6$. Therefore, there must exist a unique root of $S(\phi)=2m$, say $\phi(m)$. For such a $\phi=\phi(m)$, the scheme (2.30)–(2.31) reduces to

$$x \approx \sqrt{\frac{\sqrt{3}(k+\frac{1}{2})\pi}{2\sin 2\phi(m)\cos^2\phi(m)}},$$

$$y \approx \left(\frac{2}{3}\sqrt{\frac{\sqrt{3}(k+\frac{1}{2})\pi}{2\sin 2\phi(m)\cos^2\phi(m)}}\right)^{3/2} \sin 3\phi(m).$$

We close by noting that this theory of the asymptotic forms for zeroes of the Pearcey function cannot yet be considered complete. With the analogy of the Airy function in mind, we see that there remains the need to further extend the present work to deal with zeroes of the first order partial derivatives of P.

Acknowledgements

RBP thanks the Department of Mathematics and Computer Science at the University of Lethbridge for its hospitality during the course of these investigations.

References

[1] M.V. Berry, S. Klein, Colored diffraction catastrophes, Proc. Natl. Acad. Sci. USA 93 (1996) 2614–2619.
[2] J.N.L. Connor, P.R. Curtis, A method for the numerical evaluation of the oscillatory integrals associated with the cuspoid catastrophes: application to Pearcey's integral and its derivatives, J. Phys. A 15 (1982) 1179–1190.
[3] J.N.L. Connor, P.R. Curtis, D. Farrelly, The uniform asymptotic swallowtail approximation: practical methods for oscillating integrals with four coalescing saddle points, J. Phys. A 17 (1984) 283–310.
[4] J.N.L. Connor, D. Farrelly, Molecular collisions and cusp catastrophes: three methods for the calculation of Pearcey's integral and its derivatives, Chem. Phys. Lett. 81 (2) (1981) 306–310.
[5] D. Kaminski, Asymptotic expansion of the Pearcey integral near the caustic, SIAM J. Math. Anal. 20 (4) (1989) 987–1005.
[6] R.B. Paris, The asymptotic behaviour of Pearcey's integral for complex variables, Proc. Roy. Soc. London, Ser. A 432 (1991) 391–426.
[7] R. Wong, Asymptotic Approximations of Integrals, Academic Press, Toronto, 1989.